Journal of Water Resources and Ocean Science
2022; 11(2): 38-47
http://www.sciencepublishinggroup.com/j/wros
doi: 10.11648/j.wros.20221102.13
ISSN: 2328-7969 (Print); ISSN: 2328-7993 (Online)

Application of Numerical Modelling to Assess Wave Conditions in the Port and Wave-Induced Port Downtime

Li Weiyi, Sun Yabin, Wang Kehua, Zhang Jun

CCCC-FHDI Engineering Co., Ltd., Guangzhou City, China

Email address:
sunyb@fhdigz.com (Sun Yabin)

To cite this article:
Li Weiyi, Sun Yabin, Wang Kehua, Zhang Jun. Application of Numerical Modelling to Assess Wave Conditions in the Port and Wave-Induced Port Downtime. *Journal of Water Resources and Ocean Science*. Vol. 11, No. 2, 2022, pp. 38-47. doi: 10.11648/j.wros.20221102.13

Received: July 24, 2022; **Accepted**: September 2, 2022; **Published**: September 8, 2022

Abstract: Port infrastructures are strategic for local, regional and global economic growth and development. They play a crucial role as transportation hubs and gateways for the vast majority of goods transported around the world, linking local and national supply chains to global markets. Any significant disruption in the logistics of ports can have significant economic implications. Wave heights are the most crucial weather elements that affect port operations and result in inoperative hours. Therefore, it is of great importance to assess the wave conditions in the port and eventually evaluate the wave-induced operational downtime of the port. This study uses numerical wave modelling, including spectral wave model and Boussinesq wave model, to analyze the wave conditions in the port, and subsequently derive the wave-induced operational downtime assessed against the limiting wave height standard. Spectral and Boussinesq wave models are respectively used to simulate the wave transformation from deep sea to shallow water and wave agitation in the port basin in consideration of a variety of incident wave conditions. The transfer functions between various incident wave conditions and the wave heights in the port basin are then derived using multi-variable interpolation. Finally, the incident wave time series are transferred to the wave height time series at berths, based on which the port downtime is calculated via statistical analysis.

Keywords: Numerical Wave Simulation, Spectral Wave Model, Boussinesq Wave Model, Transfer Function, Port Downtime

1. Introduction

Ports are the infrastructure to provide safe anchorage for vessels in order to facilitate the loading and unloading operations of cargo and passengers [1]. To perform these functions, the weather conditions inside the basin must not exceed certain thresholds, which depend on the type of operation (mooring, loading or unloading) and cargo involved [2-4]. Among the different weather elements affecting port operations, wave heights inside the port basin are the sources of most inoperative hours [5]. González-Marco et al. [6] analyzed the effect of long waves on port operations via numerical model, and determined the periods of inactivity limited by an operational criterion based on the wave conditions. López et al. [7] applied artificial neural networks to evaluate wave agitation inside the basin, and assessed the wave influence on port operations against the limiting operational wave conditions. Camus et al. [8] used the metamodel to transform the wave conditions from the entrance of the harbor towards the inside port, and assessed the port operation downtime due to wave disturbance in consideration of climate change projected by a stochastic weather generator.

Numerical wave models have developed as an approximate yet reliable solution of the differential equations describing wave propagation and transformation. There are essentially two types of numerical wave models: spectral models, which provide a phase-averaged description of wave propagation, e.g., SWAN [9, 10]; and phase-resolving models, including mild slope models [11, 12] and Boussinesq models [13, 14]. The main advantage of spectral models is that they consider the generation and development of wind waves. However, the spectral models cannot resolve phenomena like diffraction or reflection for which the phase information is essential. On the contrary, the mild slope and Boussinesq models do resolve the phase, but can only be implemented in small areas given their high computational cost.

This study proposed a sophisticated method, which take advantages of both numerical spectral wave model and Boussinesq wave model, to assess the wave conditions in the

port basin and subsequently evaluate the wave-induced port downtime. Spectral wave model is used to transform the wave time series from deep sea to shallow water, whereas Boussinesq wave model is used to simulate wave agitation in the port basin in consideration of a variety of incident wave conditions. The transfer functions between various incident wave conditions and the wave heights in the port basin are derived using multi-variable interpolation, based on which long-term wave height time series in the port basin are derived and the wave-induced port downtime is accurately determined as assessed against the limiting operational wave height criteria.

The methodology is illustrated through a case study: a deep-water container port in the Mediterranean. The case study comprises of two breakwaters, the existence of which incurs strong wave diffraction phenomenon and necessitates the phase-resolving model to simulate wave agitation in the port basin. The proposed assessment methodology, model development, results and conclusions are further elaborated in the following sections.

2. Methodology

Figure 1 presents the flow diagram of the proposed assessment method for wave conditions and port downtime. The assessment method can be carried out in following steps.

Step 1. Develop spectral regional wave model to propagate the long-term wave time series from offshore to near shore; analyse and determine typical near shore wave conditions, i.e., combinations of prevailing wave height, wave period and wave direction;

Step 2. Apply Boussinesq wave model to simulate wave agitation in the port basin with input from typical near shore wave conditions; establish the transfer function between the port basin wave heights and the typical near shore wave conditions;

Step 3. Use the transfer function to convert the long-term near shore wave time series into long-term port basin wave time series; compare with the limiting operational wave height to derive the wave-induced downtime for the berths of interest.

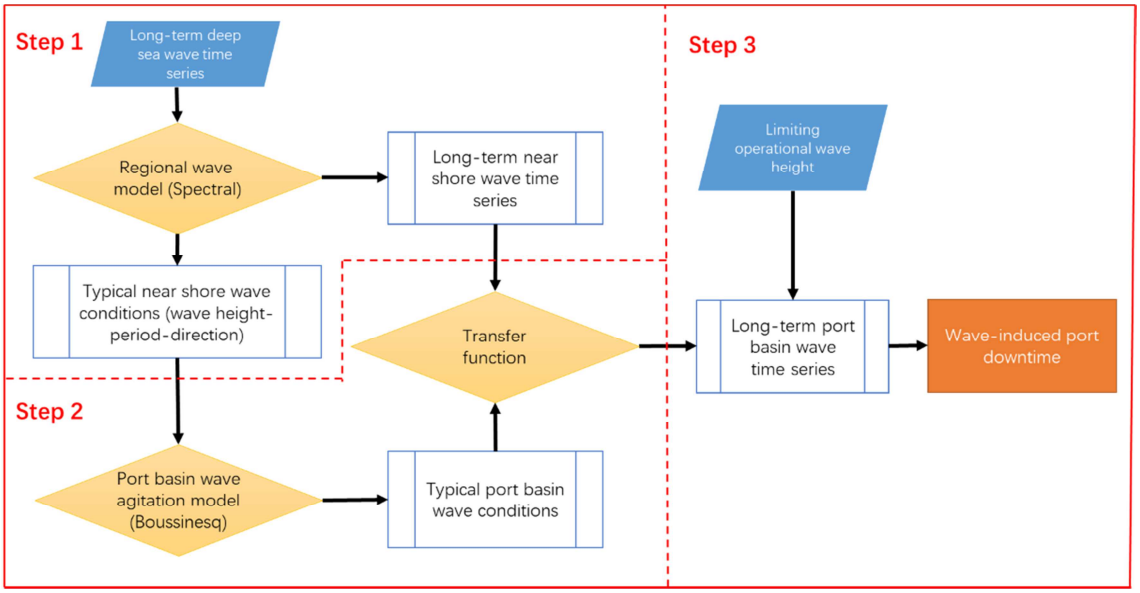

Figure 1. *Flow diagram of the proposed assessment method for wave conditions in the port and wave-induced port downtime.*

2.1. Spectral Wave Model

The governing equation for the spectral wave model is the wave action balance equation [15, 16]. Formulated in Cartesian co-ordinates, the conservation equation for wave action can be expressed as:

$$\frac{\partial N}{\partial t} + \nabla \cdot (\vec{v} N) = \frac{S}{\sigma} \tag{1}$$

where $N(\vec{x}, \sigma, \theta, t)$ is the action density, t is the time, $\vec{x} = (x, y)$ is the Cartesian co-ordinates, $\vec{v} = (c_x, c_y, c_\sigma, c_\theta)$ is the propagation velocity of a wave group in the four-dimensional phase space $\vec{x}$, σ and θ, ∇ is the four-dimensional differential operator, and S is the source term for the energy balance equation. The energy source term S represents the superposition of source functions describing various physical phenomena, i.e.,

$$S = S_{in} + S_{nl} + S_{ds} + S_{bot} + S_{surf} \tag{2}$$

where S_{in} is the generation of energy by wind, S_{nl} is the wave energy transfer due to non-linear wave-wave interaction, S_{ds} is the dissipation of wave energy due to white-capping, S_{bot} is the dissipation due to bottom friction and S_{surf} is the dissipation of wave energy due to depth-induced breaking.

Spectral wave model is competent to simulate the physical phenomena including wave growth by action of wind, non-linear wave-wave interaction, dissipation due to white-capping, dissipation due to bottom friction, dissipation due to depth-induced wave breaking, refraction and shoaling due to depth variations, etc.

2.2. Boussinesq Wave Model

Boussinesq wave model solves the Boussinesq type

equations [17-19]. The Boussinesq equations include nonlinearity as well as frequency dispersion, which is basically introduced in the momentum equations by taking into account the effect that the vertical accelerations have on the pressure distribution. Formulated in an enhanced form, the Boussinesq equations read:

$$n\frac{\partial \xi}{\partial t}+\frac{\partial P}{\partial x}+\frac{\partial Q}{\partial y}=0 \tag{3}$$

$$n\frac{\partial P}{\partial t}+\frac{\partial}{\partial x}\left(\frac{P^2}{h}\right)+\frac{\partial}{\partial y}\left(\frac{PQ}{h}\right)+\frac{\partial R_{xx}}{\partial x}+\frac{\partial R_{xy}}{\partial x}+F_x n^2 gh\frac{\partial \xi}{\partial x}+n^2 P\left[\alpha+\beta\frac{\sqrt{P^2+Q^2}}{h}\right]+\frac{gP\sqrt{P^2+Q^2}}{h^2C^2}+n\Psi_1=0 \tag{4}$$

$$n\frac{\partial Q}{\partial t}+\frac{\partial}{\partial y}\left(\frac{Q^2}{h}\right)+\frac{\partial}{\partial x}\left(\frac{PQ}{h}\right)+\frac{\partial R_{yy}}{\partial y}+\frac{\partial R_{xy}}{\partial y}+F_y n^2 gh\frac{\partial \xi}{\partial y}+n^2 Q\left[\alpha+\beta\frac{\sqrt{P^2+Q^2}}{h}\right]+\frac{gQ\sqrt{P^2+Q^2}}{h^2C^2}+n\Psi_2=0 \tag{5}$$

where ξ is the free surface elevation, P, Q are the flux density in the x-direction and y-direction respectively, n represents the porosity, t is the time, x, y are the Cartesian co-ordinates, h is the total water depth, R_{xx}, R_{xy} and R_{yy} account for the excess momentum originating from the non-uniform velocity distribution, F_x and F_y are the horizontal stress term in the x-direction and y-direction respectively, g is the gravitational acceleration, α is the resistance coefficient for laminar flow in porous media, β is the resistance coefficient for turbulent flow in porous media, C is the Chezy resistance number, Ψ_1 and Ψ_2 are the Boussinesq dispersion terms.

Boussinesq wave model is capable of reproducing the combined effects of important wave phenomena, including shoaling, refraction, diffraction, wave breaking, partial reflection and transmission, non-linear wave-wave interaction, frequency spreading, direction spreading, etc.

3. Model Development and Results

3.1. Study Case

The proposed assessment scheme is applied to a deep-water container port in the Mediterranean. The container port is in the planning and design stage, yet it serves as an interesting study case attributed to its unique location and layout design.

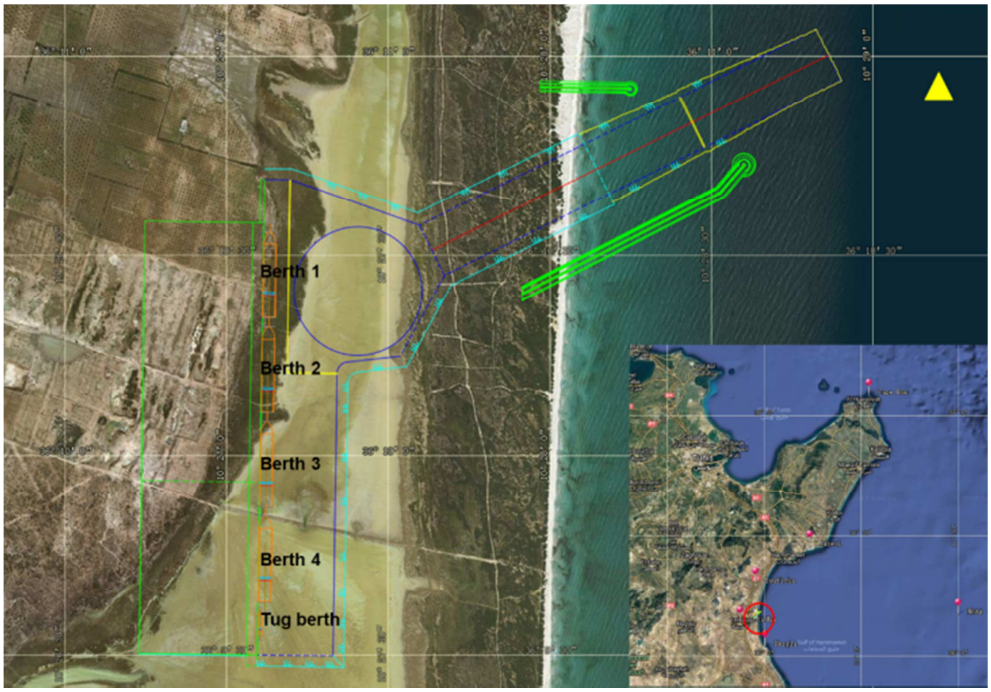

Figure 2. *Geographical location and general layout of the container port (Red circle: project site; yellow rectangle: spectral wave information extraction point).*

Figure 2 shows the location and general layout of the container port. The port is located in Gulf of Hammamet, and is primarily composed of north breakwater, south breakwater, access channel, turning basin, 4 container berths and 1 tug berth.

3.2. Regional Wave Model

Figure 3 shows the model extent, bathymetry and grid of the regional wave model. The regional wave model covers the entire Gulf of Hammamet, with the eastern open boundary located at 11.5°E. The model domain is large enough to allow accurate representation of wave propagation and transformation in the study area. The bathymetry is generated from the digital nautical chart, combined with the surveyed bathymetric data at the coastal area. The regional wave model uses a flexible triangular mesh with progressively increasing spatial resolutions towards the project site. The depth-adaptive mesh has a resolution of 10 km at the open boundary and 20 m at the project site.

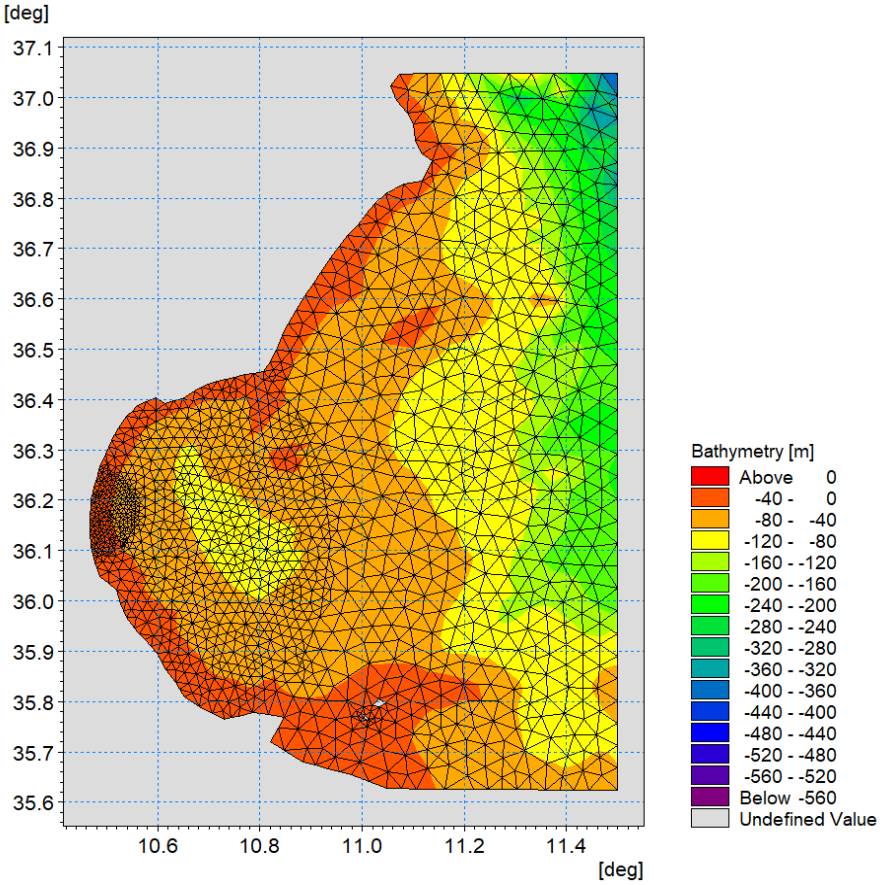

Figure 3. *Model extent, bathymetry and grid for the regional wave model.*

Table 1 summaries the essential model parameter setup for the regional wave model. A fully spectral formulation is applied with a logarithmic frequency discretization, formulated as:

$$f_n = f_0 c^n, \ n = 1,2, \ldots \quad (6)$$

where f_n is the frequency, f_0 is the minimum frequency (0.055 Hz), c is the frequency factor (1.1), and n is the number of frequencies (25). Values in brackets are adopted in this study, implying a frequency range of (0.055Hz, 0.6Hz), or equivalently a period range of (0.6s, 18.2s). The directional discretization is set as a 360-degree rose, with number of directions of 16.

Table 1. *Summary of essential parameters in regional wave model setup.*

Settings	**Regional wave model**
Grid resolution	20m~10km
Governing equation	Fully spectral
Spectral discretization	25 frequencies (0.055Hz, 0.6Hz); 16 directions from 0° to 360°
Simulation period	1979-2017
Time step	Min: 0.01 s; Max: 30 s
Water level	Tidal variation
Wave breaking	Limiting wave steepness γ=0.8
Bottom friction	Nikuradse roughness kn=0.001m
White-capping	Dissipation coefficient Cdis=4.5, DELTA dis=0.5
Wind forcing	CFSR wind
Boundary conditions	FHDI Global Normal Wave Model (FHDI-GNWM)

The model boundaries are prescribed as temporally varying wave parameters obtained from the FHDI Global Normal Wave Model (FHDI-GNWM) [20]. The model is driven by temporally varying CFSR wind forcing [21] and temporally varying water levels predicted from the tidal station. The hindcast regional wave data are established for 39 years covering the period from 1979 to 2017 with a one-hour temporal resolution. The model output includes integrated sea-state parameters, such as the significant wave height H_{m0}, peak wave period T_p and mean wave direction MWD, as well as wave spectral information within the entire model domain.

Wave parameters are extracted from the regional wave model and analyzed at the reference point in front of breakwater at -20m isobath, as marked by the yellow triangle

in Figure 2. Figure 4 shows the wave rose at the extraction point, whereas Table 2 and Table 3 respectively present the scatter tables of significant wave height H_{m0}, vs. mean wave direction MWD and significant wave height H_{m0} vs. peak wave period T_p. Most waves come from NNE, NE, ENE, E, ESE and SE with a cumulative frequency of 96.14, and most peak wave period T_p ranges between 2 to 10 s with a cumulative frequency of 98.89%.

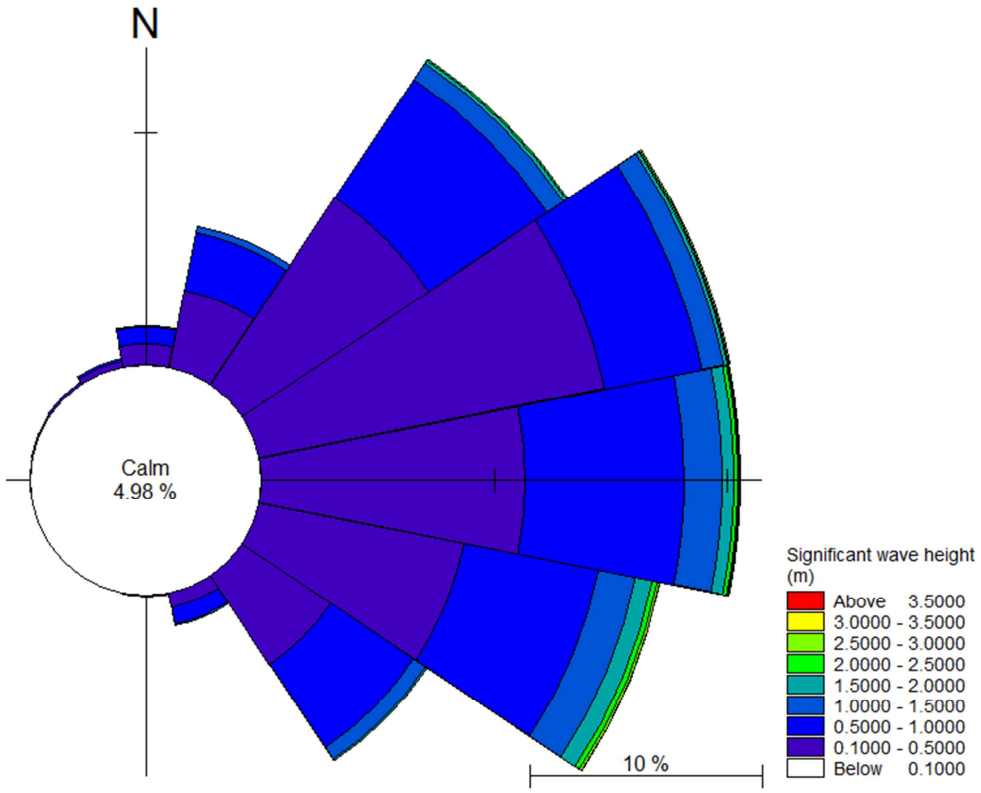

Figure 4. *Wave rose at the extraction point.*

Ultimately every time step from the long-term wave time series should be modelled also in the subsequent wave agitation model by applying the exact spectral properties from the wave transformation model. However, this is far from being feasible as the 39-year time series contain more than 300,000 values. Therefore, the wave agitation simulations are limited to a feasible number of representative simulations, where certain choices on spectral shape and directional spreading are made. In order to encompass the relevant wave conditions, a total of 18 incident wave scenarios are considered in the wave agitation simulation as summarized in Table 4. The incident wave scenarios include 1 significant wave height H_{m0} of 1 m, 3 peak wave period T_p: 3, 6, 9 s, and 6 mean wave direction MWD: NNE, NE, ENE, E, ESE, SE.

Table 2. *Wave scatter table for frequency of occurrence at the extraction point: significant wave height H_{m0} vs. mean wave direction MWD.*

Direction	Significant wave height (m)								
	0-0.5	0.5-1	1-1.5	1.5-2	2-2.5	2.5-3	3-3.5	>3.5	Total
N (348.75-360-11.25)	0.91	0.72	0.03	0.00	0.00	0.00	0.00	0.00	1.66
NNE (11.25-22.5-33.75)	3.65	2.53	0.29	0.02	0.00	0.00	0.00	0.00	6.49
NE (33.75-45-56.25)	11.59	6.12	0.85	0.18	0.02	0.00	0.00	0.00	18.76
ENE (56.25-67.5-78.75)	16.22	4.26	0.95	0.20	0.05	0.01	0.00	0.00	21.70
E (78.75-90-101.25)	11.72	6.88	1.63	0.49	0.18	0.06	0.02	0.02	21.00
ESE (101.25-112.5-123.75)	9.48	5.86	1.65	0.71	0.23	0.11	0.03	0.01	18.08
SE (123.75-135-146.25)	5.12	4.28	0.64	0.08	0.00	0.00	0.00	0.00	10.11
SSE (146.25-157.5-168.75)	0.73	0.71	0.06	0.00	0.00	0.00	0.00	0.00	1.50
S (168.75-180-191.25)	0.04	0.04	0.00	0.00	0.00	0.00	0.00	0.00	0.07
SSW (191.25-202.5-213.75)	0.01	0.00	0.00	0.00	0.00	0.00	0.00	0.00	0.02
SW (213.75-225-236.25)	0.01	0.00	0.00	0.00	0.00	0.00	0.00	0.00	0.01
WSW (236.25-247.5-258.75)	0.02	0.00	0.00	0.00	0.00	0.00	0.00	0.00	0.02
W (258.75-270-281.25)	0.02	0.00	0.00	0.00	0.00	0.00	0.00	0.00	0.03
WNW (281.25-292.5-303.75)	0.04	0.00	0.00	0.00	0.00	0.00	0.00	0.00	0.05
NW (303.75-315-326.25)	0.10	0.01	0.00	0.00	0.00	0.00	0.00	0.00	0.11
NNW (326.25-337.5-348.75)	0.26	0.12	0.00	0.00	0.00	0.00	0.00	0.00	0.38
Total	59.91	31.55	6.10	1.67	0.49	0.19	0.06	0.03	100.00

Table 3. *Wave scatter table for frequency of occurrence at the extraction point: significant wave height H_{m0} vs. peak wave period T_p.*

Peak wave period (s)	Significant wave height (m)								
	0-0.5	**0.5-1**	**1-1.5**	**1.5-2**	**2-2.5**	**2.5-3**	**3-3.5**	**>3.5**	**Total**
0-2	0.46	0.00	0.00	0.00	0.00	0.00	0.00	0.00	0.46
2-4	27.40	6.45	0.04	0.00	0.00	0.00	0.00	0.00	33.89
4-6	24.08	13.58	2.16	0.26	0.01	0.00	0.00	0.00	40.09
6-8	6.67	9.41	2.55	0.89	0.28	0.08	0.01	0.00	19.90
8-10	1.08	1.96	1.16	0.46	0.19	0.10	0.04	0.02	5.01
10-12	0.20	0.15	0.19	0.07	0.01	0.01	0.01	0.01	0.65
>12	0.01	0.00	0.00	0.00	0.00	0.00	0.00	0.00	0.01
Total	59.91	31.55	6.10	1.67	0.49	0.19	0.06	0.03	100.00

Table 4. *Summary of incident wave scenarios.*

No.	H_{m0} (m)	T_p (s)	MWD (°N)
1	1	3	22.5
2	1	6	22.5
3	1	9	22.5
4	1	3	45
5	1	6	45
6	1	9	45
7	1	3	67.5
8	1	6	67.5
9	1	9	67.5
10	1	3	90
11	1	6	90
12	1	9	90
13	1	3	112.5
14	1	6	112.5
15	1	9	112.5
16	1	3	135
17	1	6	135
18	1	9	135

By using a boundary condition with 1 m significant wave height H_{m0}, the wave conditions determined in the port basin can be viewed as wave disturbance coefficients, i.e., defining the wave height relative to the incident wave height. Hence, if a different incident wave height (but with same wave direction and wave period) is used at the boundary, the corresponding wave heights in the port basin are derived by multiplying the incident wave height and the wave disturbance coefficients. A prerequisite for this approach is that the non-linear wave effects are insignificant, which is the case in the present study where the water depths are relatively large compared to the wave heights so that wave breaking is not important.

3.3. Wave Agitation Model

Figure 5 shows the model extent, bathymetry, internal wave generation line and reflection characteristics of the wave agitation model. The model extent covers the entire container port, with the eastern boundary located at isobath of -25 m. The model bathymetry is derived from the digital nautical chart, the surveyed bathymetric data at the coastal area, and the designed water depth at the port area. The internal wave generation line is located at -20 m, where the incident wave information is extracted from the regional wave transformation model and prescribed to the wave agitation model. All the model boundaries, except for the port interior and beach, are modelled as wave absorbing, meaning that all wave energy reaching these model boundaries is absorbed to prevent waves from being reflected back into the model domain. Partial reflection is applied along the beach, breakwater, revetment and quay wall, where the reflection characteristics are estimated from the type of structure and local wave conditions, as shown in Figure 5.

Directional irregular waves with corresponding significant wave height H_{m0}, peak wave period T_p, and mean wave direction MWD, as summarized in Table 4, are applied for defining the incident wave conditions in the scope of wave agitation simulation. The spectral shape and directional spreading applied for the boundary conditions are based on the results from the wave transformation model. It reveals that the incident waves can be represented by a JONSWAP spectrum with a peak enhancement factor (γ) of 3.3 and the directional standard deviation (DSD) is in the order of 10°-15°.

The water level has little influence on wave agitation, which is thus set to 0m mean sea level (MSL) in the agitation model. The duration of the wave agitation simulation corresponded to 45 minutes, of which the first 15 minutes are used for model warm-up and the last 30 minutes are used for computation of the wave disturbance coefficients.

Examples of snapshots of the wave agitation simulation are presented in Figure 6, and Table 5 summarizes the disturbance coefficients at the 4 berths corresponding to the incident wave scenarios. The largest disturbance coefficients come from wave direction of 67.5°N, i.e., Scenario 7, 8 and 9, when the wave direction is almost in parallel with the direction of approach channel and most wave energy can propagate into the port basin. For the more oblique wave directions, e.g., 22.5 and 135°N, the disturbance coefficients are minute attributed to the sheltering effect from the breakwater.

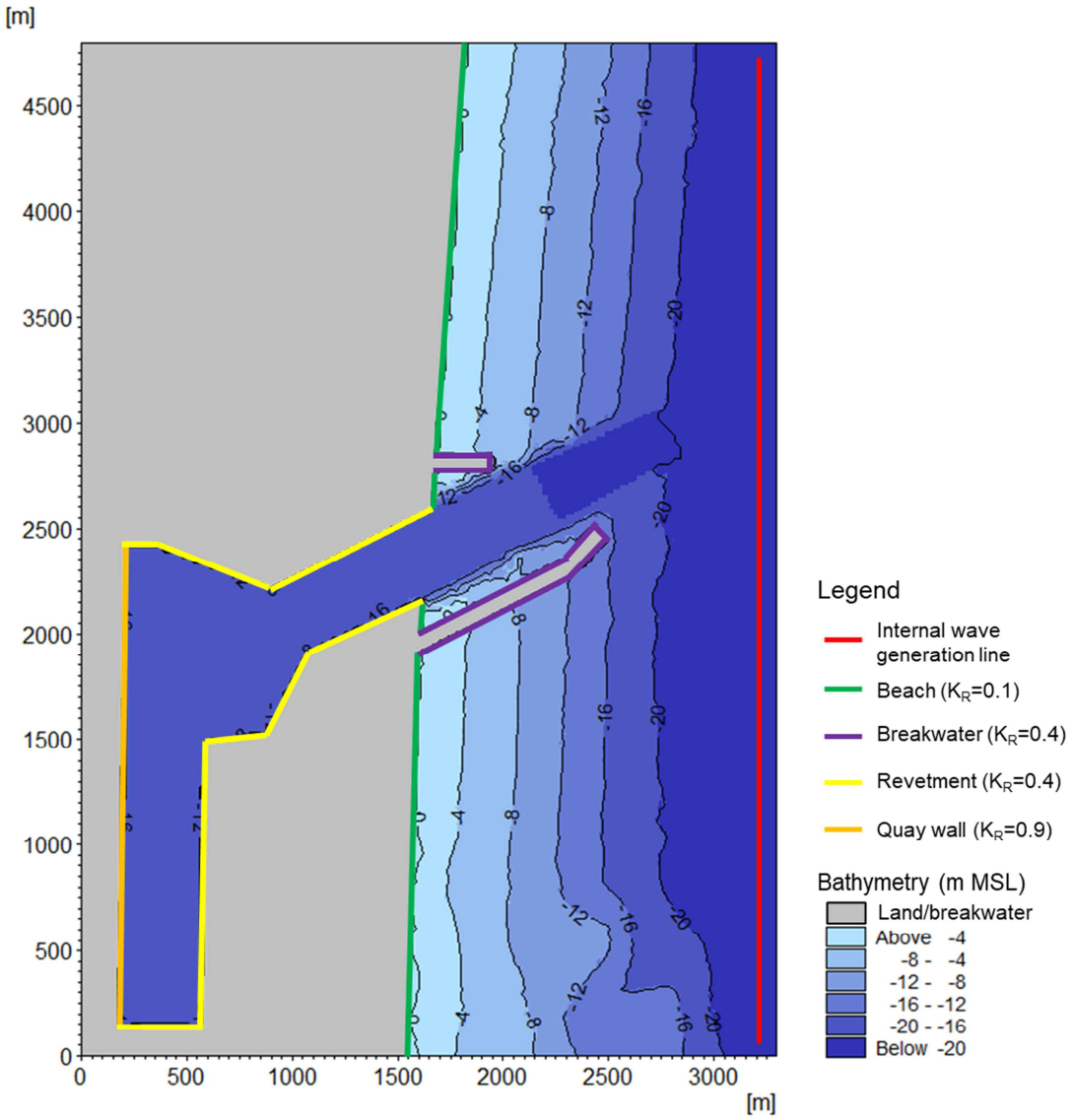

Figure 5. *Model extent, bathymetry, internal wave generation line and reflection characteristics (K_R: wave reflection coefficient) for the wave agitation model.*

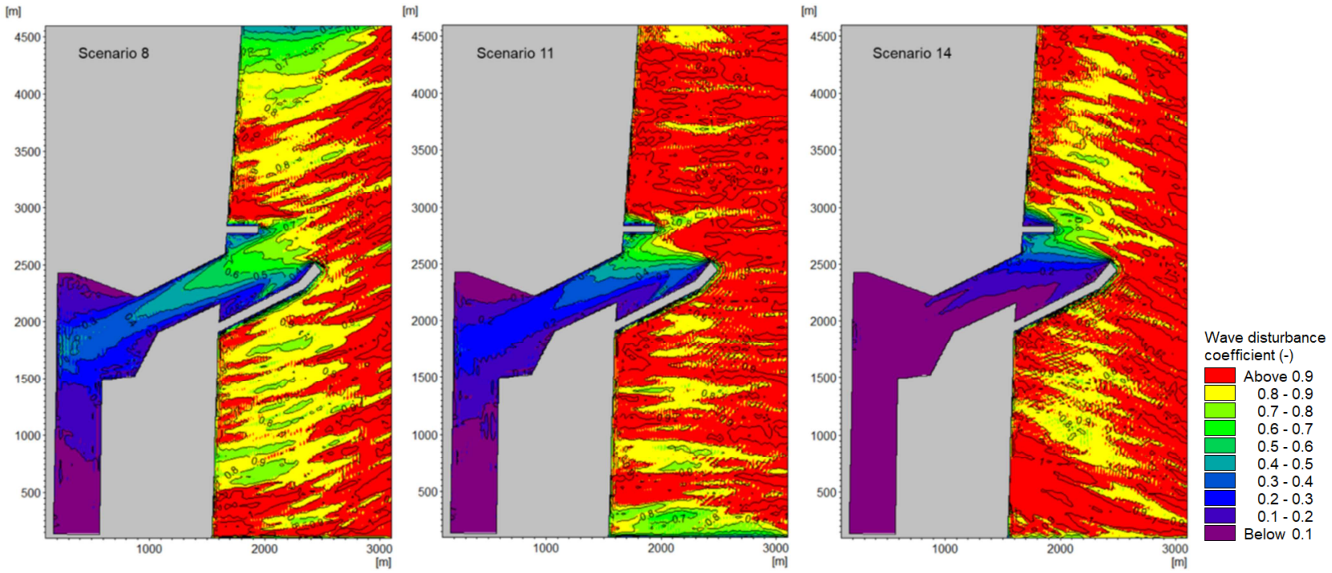

Figure 6. *Snapshots of wave agitation simulation (Scenario 8, 11 and 14: Hs = 1m, Tp = 6s, MWD = 67.5°N, 90°N and 112.5°N).*

Table 5. *Disturbance coefficients at the 4 berths.*

No.	Berth 1	Berth 2	Berth 3	Berth 4
1	0.013	0.004	0.004	0.002
2	0.078	0.175	0.056	0.050
3	0.052	0.047	0.065	0.047
4	0.017	0.010	0.005	0.004
5	0.183	0.275	0.077	0.064
6	0.108	0.068	0.101	0.077
7	0.040	0.014	0.006	0.004
8	0.354	0.288	0.090	0.072
9	0.150	0.101	0.119	0.108
10	0.041	0.012	0.006	0.004
11	0.256	0.222	0.063	0.057
12	0.094	0.068	0.090	0.080
13	0.021	0.006	0.004	0.004
14	0.101	0.054	0.023	0.024
15	0.041	0.026	0.037	0.034
16	0.003	0.000	0.000	0.000
17	0.031	0.022	0.016	0.017
18	0.032	0.022	0.029	0.031

3.4. Assessment Results

Based on the wave agitation simulation, the transfer functions between the incident wave time series and the wave heights in the port basin can be derived. The transfer functions at the 4 berths are plotted in Figure 7, which can be formulated as

$$H_i = f_i\left(H_{m0}, T_p, MWD\right)\ (i = 1,2,\cdots,4) \qquad (7)$$

where $H_1 \sim H_4$ represent the wave heights at the 4 berths, H_{m0}, T_p and MWD are respectively the significant wave height, peak weak period and mean wave direction of the incident waves, $f_1 \sim f_4$ are the transfer functions. As the incident significant wave height H_{m0} is selected as 1 m, the wave heights $H_1 \sim H_4$ also represent the wave disturbance coefficients at the 4 berths. In case of a different incident wave height but with same wave direction and wave period, the actual wave heights at the berths can be derived by multiplying the incident wave height and the respective wave disturbance coefficients $H_1 \sim H_4$.

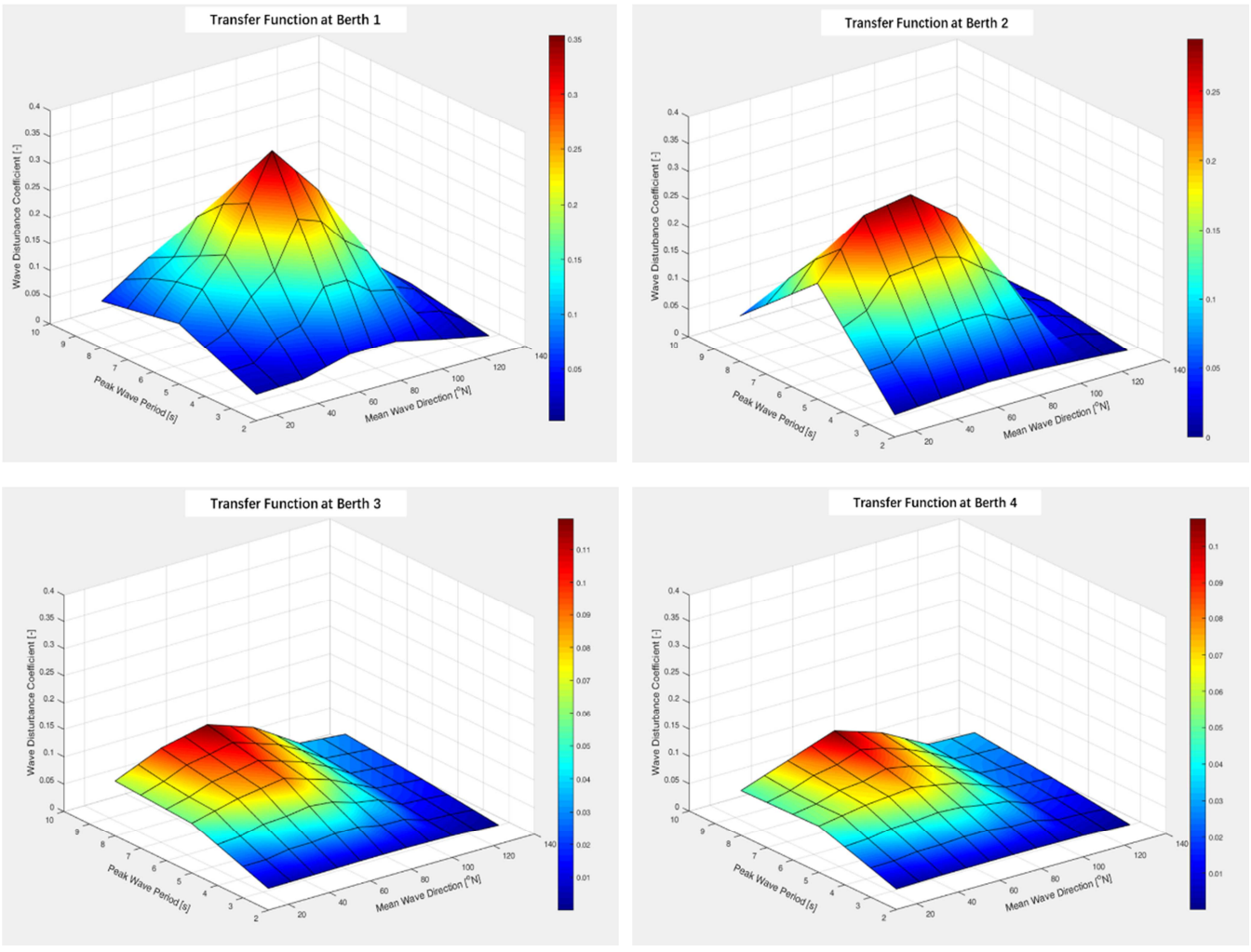

Figure 7. *Transfer functions at the 4 berths.*

The transfer functions, with the input from incident wave information, are applied to derive the wave height time series at the 4 berths. Figure 8 shows an example of the transferred wave height time series and its cumulative frequency distribution curve at berth 1. Following the PIANC recommendation [22], the limiting operational wave height criteria are adopted as H_{m0} = 0.5 m for the container berth. From the cumulative frequency distribution curve, it can be observed that the cumulative frequency for H_{m0} = 0.5 is 0.30%, implying the wave-induced downtime at berth 1 corresponds to 0.30%.

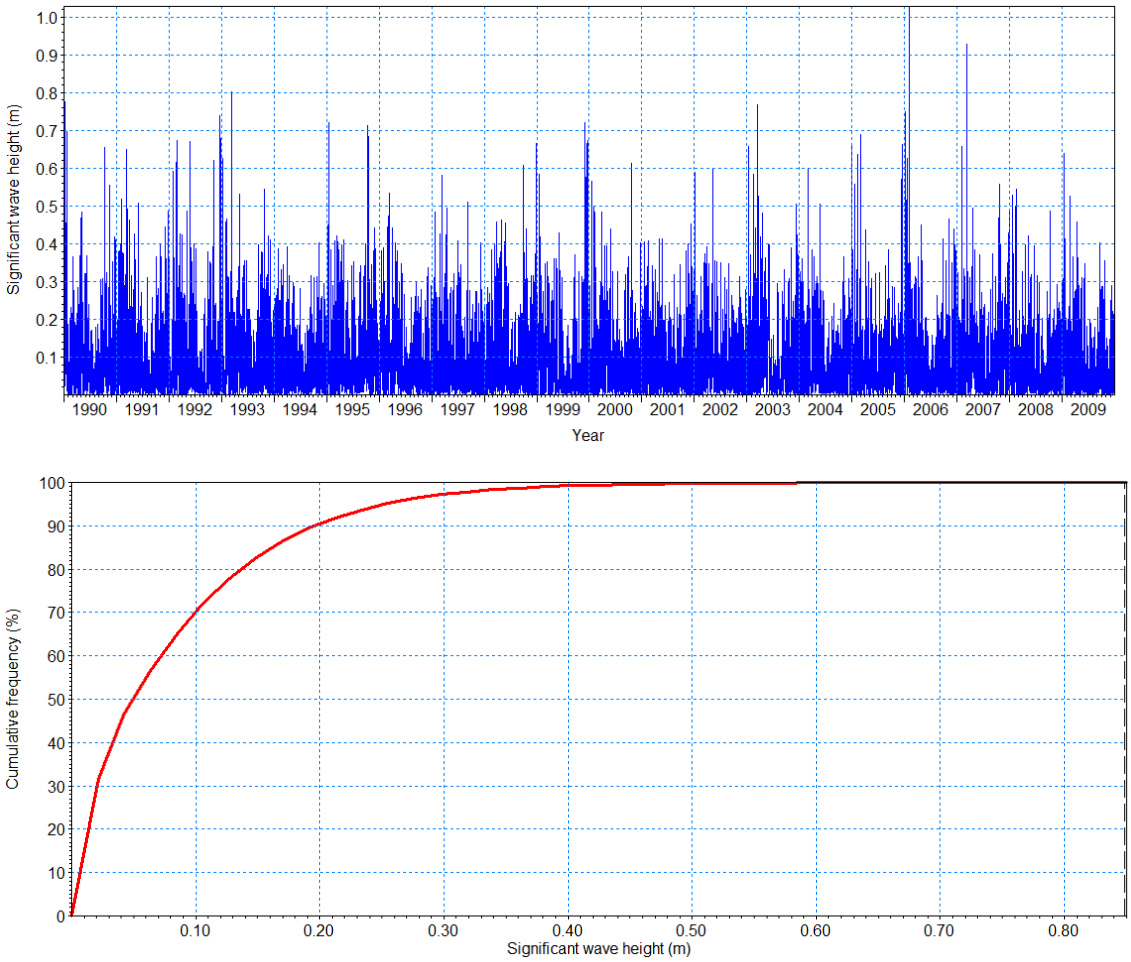

Figure 8. *Wave height time series and cumulative frequency distribution curve at Berth 1.*

Table 6 summarizes the downtime estimated for the 4 berths. Berth 1 appears to be the most exposed berth, while the downtime reduces to 0.01% at Berth 4. The downtime assessment is averaged based on the 39 years of data, and there will be variations from year to year. Nevertheless, the estimated downtime is far below the recommended value of 2% for the container port as in the PIANC guideline [23].

Table 6. *Downtime assessment for the 4 berths.*

Berth 1	Berth 2	Berth 3	Berth 4
0.30%	0.25%	0.10%	0.01%

4. Conclusions

A sophisticated method to assess the wave conditions in the port basin and the wave-induced port downtime is proposed and elaborated in this study. The assessment method combines the numerical spectral wave modelling with Boussinesq wave modelling. The spectral wave model is used to investigate the wave propagation and transformation from deep sea to near shore, and the Boussinesq wave model is to simulate the wave agitation in the port basin. In order to make the wave agitation simulation feasible, the wave time series are extracted from the spectral wave model and analyzed at the reference point in front of the breakwater, resulting in 18 representative incident wave scenarios. Transfer functions are derived based on the numerical wave simulation results, which are then applied to convert the incident wave time series into wave height time series at berths. The port downtime is finally estimated as assessed against the criteria.

The proposed method is applied to a deep-water container port in the Mediterranean. The results reveal that the northernmost berth, i.e., Berth 1, is the most exposed berth with the largest downtime, while the wave condition improves and downtime reduces when it moves to south. The downtime at Berth 1, 2, 3 and 4 are respectively 0.3%, 0.25%,

0.10%, 0.01%, which are far below the recommended downtime of 2% for the container port.

This study systematically demonstrates a general procedure of assessing the wave conditions in the port basin and the wave-induced downtime using numerical wave modelling. This procedure can be applied to any actual port-design projects of similar type, and is of great value for the engineering design and optimization practice.

References

[1] Goda, Y., 2002. Random Seas and Design of Maritime Structures. World Scientific, Singapore.

[2] Elzinga, T., Iribarren, J. R., Jensen, O. J., 1992. Movements of moored ships in harbours. In: Proceedings of the 23rd International Conference on Coastal Engineering, 3216–3229.

[3] PIANC, 1995. Criteria for Movements of Moored Ships in Harbours: A Practical Guide. Permanent International Association of Navigation Congresses. Permanent Technical Committee II. Working Group 24, Brussels, Belgium.

[4] Puertos del Estado, 1999. ROM 3.1-99: Recommendations for the Design of the Maritime Configuration of Ports, Approach Channels and Harbour Basins. Spanish Ministry of Public Works, Madrid, Spain.

[5] Tsinker, G. P., 2004. Port Engineering: Planning, Construction, Maintenance, and Security. John Wiley & Sons, Hoboken, New Jersey.

[6] González-Marco, D., Sierra, J. P., Fernández de Ybarra, O., Sánchez-Arcilla, A., 2008. Implications of long waves in harbor management: the Gijón port case study. Ocean & Coastal Management 51 (2), 180–201.

[7] López, I., López, M., Iglesias, G., 2015. Artificial neural networks applied to port operability assessment. Ocean Engineering 109, 298-308.

[8] Camus, P., Tomás, A., Díaz-Hernández, G., Rodríguez, B., Izaguirre, C., Losada, I. J., 2019. Probabilistic assessment of port operation downtimes under climate change. Ocean Engineering 147, 12-24.

[9] Rusu, E., Guedes Soares, C., 2011. Wave modelling at the entrance of ports. Ocean Enginerring 38 (17–18), 2089–2109.

[10] Rusu, L., Guedes Soares, C., 2013. Evaluation of a high-resolution wave forecasting system for the approaches to ports. Ocean Engineering 58, 224–238.

[11] Chen, W., Panchang, V., Demirbilek, Z., 2005. On the modelling of wave–current interaction using the elliptic mild-slope wave equation. Ocean Engineering 32 (17–18), 2135–2164.

[12] Hamidi, M. E., Hashemi, M. R., Talebbeydokhti, N., Neill, S. P., 2012. Numerical modelling of the mild slope equation using localised differential quadrature method. Ocean Engineering 47, 88–103.

[13] Bruno, D., De Serio, F., Mossa, M., 2009. The FUNWAVE model application and its validation using laboratory data. Coastal Engineering 56 (7), 773–787.

[14] Su, S.-F., Ma, G., Hsu, T.-W., 2015. Boussinesq modelling of spatial variability of infragravity waves on fringing reefs. Ocean Engineering 101, 78–92.

[15] Komen, G. J., Cavaleri, L., Doneland, M., Hasselmann, K., Hasselmann, S., Janssen, P. A. E. M., 1994. Dynamics and Modelling of Ocean Waves. Cambridge University Press, UK.

[16] Young, I. R., 1999. Wind Generated Ocean Waves. Elsevier Ocean Engineering Book Series, Volume 2, Elsevier.

[17] Madsen, P. A., Murray, R., Sørensen, O. R, 1991. A new form of the Boussinesq equations with improved linear dispersion characteristics. Coastal Engineering 15 (4), 371-388.

[18] Madsen, P. A., Sørensen, O. R., 1992. A new form of the Boussinesq equations with improved linear dispersion characteristics. Part 2. A slowly-varying bathymetry. Coastal Engineering 18 (3-4), 183-204.

[19] Sørensen, O. R., Schäffer, H. A., Sørensen, L. S, 2004. Boussinesq-type modelling using an unstructured finite element technique. Coastal Engineering 50 (4), 181-198.

[20] CCCC-FHDI, 2022. Analysis and Calculation Guideline for Meteorological and Hydrological Conditions of Sea Port Based on the Chinese and International Codes and Standards. China Communications Construction Company, Fourth Harbour Design Institute. Beijing, China.

[21] Kanamitsu, M., Ebisuzaki, W., Woollen, J., Yang, S. K., Hnilo, J. J., Fiorino, M., 2002. NCEP–DOE AMIP-II Reanalysis (R-2). Bulletin of the American Meteorological Society 83 (11), 1631–1644.

[22] PIANC, 2014. Harbour Approach Channels Design Guidelines. Permanent International Association of Navigation Congresses. Maritime Navigation Commission. Working Group 49, Brussels, Belgium.

[23] PIANC, 2012. Criteria for the (Un) loading of Container Vessels. Permanent International Association of Navigation Congresses. Maritime Navigation Commission. Working Group 115, Brussels, Belgium.